EDGE ARTICLE

Check for updates

para-Selective dearomatization of phenols by I(I)/I(III) catalysis-based fluorination†

Timo Stünkel, Kathrin Siebold, [ID] Daichi Okumatsu, Kazuki Murata, Louise Ruyet, [ID] Constantin G. Daniliuc [ID] and Ryan Gilmour [ID] *

The regio- and enantio-selective dearomatization of phenols has been achieved by I(I)/I(III) catalysis enabled fluorination. The process is highly *para*-selective, guiding the fluoride nucleophile to the distal C4 position of the substrate to generate fluorinated cyclohexadienones in an operationally simple manner. Extensive optimization has revealed key parameters that orchestrate enantioselectivity in this historically challenging transformation. A range of diversely substituted substrates are disclosed (20 examples, up to 92 : 8 e.r.) and the reaction displays efficiency that is competitive with the current state of the art in hydroxylation chemistry: this provides a preparative platform to enable OH to F bioisosterism to be explored. Finally, the utility of the products in accessing densely functionalized cyclic scaffolds with five contiguous stereocenters is disclosed together with crystallographic analyses to unveil fluorine-carbonyl non-covalent interactions.

Introduction

The prevalence of cyclohexadienones in the bioactive small molecule repertoire has created a powerful impetus to develop effective dearomatization strategies to facilitate direct access from abundant aromatic precursors.[1] Striking examples that illustrate the functional diversity of this natural product class include the anti-thrombic agent (+)-rishirilide B (**1**),[2] the anti-inflammatory rengyolone (**2**),[3] and the mammalian DNA polymerase inhibitor dehydroaltenusin (**3**).[4] Function-driven synthesis has also fuelled the development of synthetic (fluorinated) steroids such as the key anti-inflammatory drugs dexamethasone, halometasone and diflupredante (**4–6**):[5] the former (**4**) is listed in the World Health Organisation's list of essential medicines.[6] The remarkable success of fluorinated cyclohexadienones in pharmaceutical development stems from Fried and co-workers studies on cortisol and prednisolone fluorination in the late 1950s.[7] Consequently, efficient strategies to generate these important APIs continue to be intensively pursued.[5] The societal importance of fluorinated cyclohexadienones led us to explore the feasibility of a C4-regioselective dearomatization of phenols to directly access this class of materials (Scheme 1A). Cognizant of the importance of fluorine in medicinal chemistry and the potency of F to OH bioisosterism,[8] it was envisaged that this transformation would be highly enabling and address a deficiency in the

synthesis arsenal. To the best of our knowledge, enantioselective I(I)/I(III)-catalysis paradigms to achieve dearomatization at C4 selectively are conspicuously underdeveloped.[9] Indeed, the process is limited to stoichiometric racemic protocols using either PIDA/PIFA with Olah's reagent,[10] or with Selectfluor® or Accufluor™.[11] Whilst this C4 selective variant has proven recalcitrant, I(I)/I(III) catalysis manifolds have a venerable history in the asymmetric dearomatization of phenols. This has enabled a broad range of diverse transformations to be executed with high levels of selectivity, whilst mitigating the need for metal catalysts. However, an important caveat that must be considered in enantioselective reaction development is the formation of phenoxenium cations through the I(III)-mediated oxidation of the phenol, which triggers a competing racemic side reaction.[14]

Inspired by the hydroxylation-based dearomatization by Maruoka and co-workers (Scheme 1B),[12] and the C4 selective fluorination of bicyclic phenols by Toste and co-workers using Selectfluor® under phase-transfer catalysis conditions (Scheme 1C)[13,15] we initiated a study to explore the causative factors that orchestrate enantioinduction (Scheme 1D).
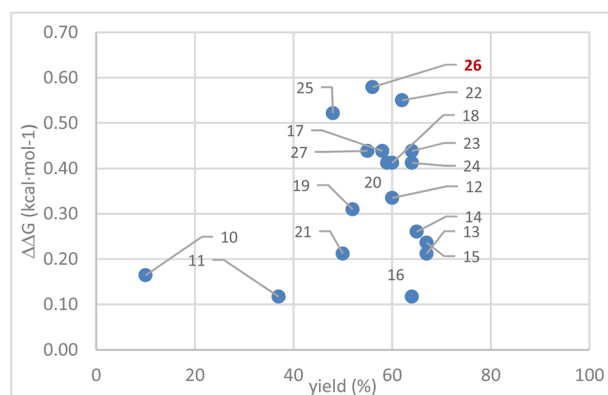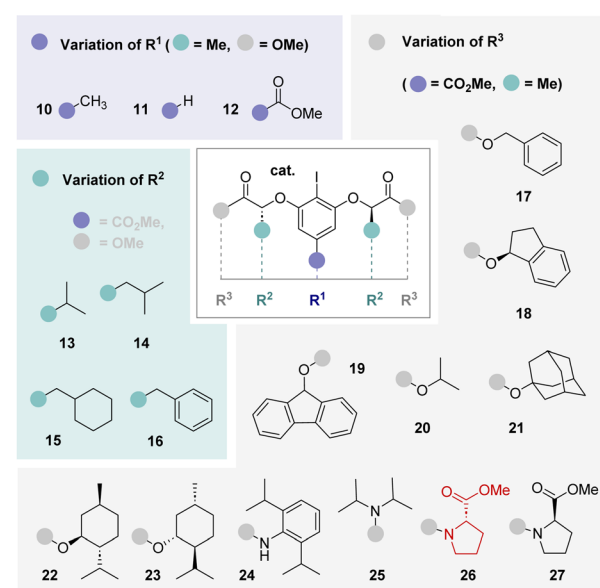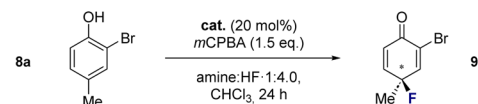
Results and discussion

To explore if the I(I)/I(III) protocol was regioselective for the C4 fluorinated isomer over the C2 species, compound **8a** was selected as the model substrate for optimization. Reaction conditions that utilized pTolI as an inexpensive organocatalyst were employed,[16] thereby enabling pTolIF$_2$ to be generated *in situ* upon oxidation.[17] A systematic study of the reaction conditions identified m-CPBA, CHCl$_3$ and an amine : HF ratio of

Organisch-Chemisches Institut, Universität Münster, Corrensstraße 36, 48149 Münster, Germany. E-mail: ryan.gilmour@uni-muenster.de
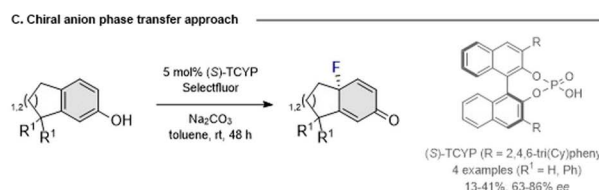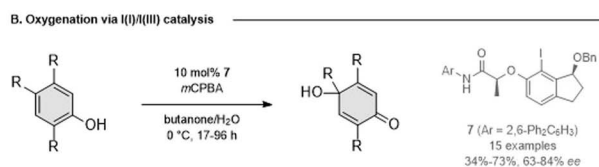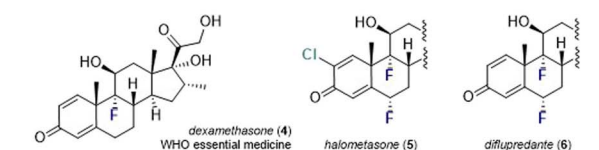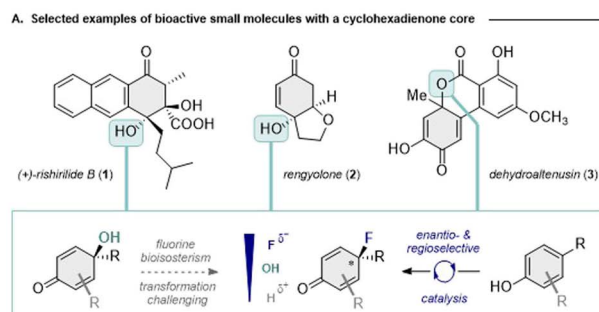
1 : 4.0 to deliver the desired C4 isomer most effectively (please see the ESI† for full details). Variation in the amine : HF ratio proved to be detrimental, with lower ratios leading to sluggish reaction rates, whereas higher ratios led to decomposition and compromised yields. With a racemic, catalysis-based protocol having been established, attention was then focused on rendering the process enantioselective (Scheme 2. Please see the plot of $\Delta\Delta G$ versus yield).

Using a lactate-based resorcinol core, a process of catalyst editing was conducted beginning with modification of the para position. This revealed a trend in efficiency that followed order p-H (**11**) < p-Me (**10**) < p-CO$_2$Me (**12**), with the latter catalyst delivering product **9a** with an enantiomeric ratio of 64 : 36 and a yield of 60%. The influence of modifications to the pendant lactate chain (**13–15**) were then investigated through a gradual

Scheme 1 (A) Selected examples of cyclohexadienones in bioactive small molecules. (B) Dearomative hydroxylation of phenols under I(ɪ)/I(ɪɪɪ) catalysis conditions by Maruoka and co-workers.[12] (C) Dearomative fluorination of phenols under phase-transfer conditions by Toste and co-workers.[13] (D) Overview of the C4-selective dearomatization of phenols under an I(ɪ)/I(ɪɪɪ) catalysis manifold.

Entry	Solvent	Additive	Temperature (°C)	Yield (%)	e.r.
1	CHCl$_3$	MeOH	rt	40%	80:20
2	CHCl$_3$	EtOH	rt	36%	79:21
3	CHCl$_3$	HFIP	rt	38%	67:33
4	Et$_2$O	-	rt	55%	80:20
5	MTBE	-	rt	52%	82:18
6	1,4-Dioxane	-	rt	51%	65:35
7	MTBE	-	0 °C	34%	88:12
8	MTBE[a]	-	0 °C	48%	88:12
9	MTBE[a,b]	-	0 °C	61%	86:14
10	MTBE[a,b]	-	-5 °C	61%	87:13
11	MTBE[a,c]	-	-5 °C	48%	90:10
12	MTBE[a,b]	-	-10 °C	45%	88:12

Scheme 2 Catalyst and reaction optimization for the title dearomatization. Standard reaction conditions: phenol (0.2 mmol), catalyst ArI (20 mol%), amine : HF 1 : 4.0 (0.5 mL), CHCl$_3$ (0.5 mL) and mCPBA (0.3 mmol), 24 h, rt. Yield was determined by ^{19}F NMR using ethyl-fluoroacetate as the internal standard. Enantiomeric ratio (e.r.) was determined by chiral HPLC.[a]Performed with 4.0 eq. mCPBA. [b]Performed with 0.35 mL of solvent and 0.65 mL amine : HF 1 : 4.0. [c]Performed with 0.75 mL of solvent and 0.25 mL of amine : HF 1 : 4.0.

increase in steric bulk. Unfortunately, these alterations led to a slight decrease in enantioselectivity relative to the parent structure **12**. Moreover, the introduction of an aromatic Bn (**16**) moiety also proved detrimental.

The terminal position of the lactate chain was then adjusted through the introduction of various esters and amides (**17–27**): this was expedited through the development of a novel route to the free diacid of the catalyst *via* the *t*Bu-ester (please see the ESI† for full details). Gratifyingly, the inclusion of an aromatic benzyl moiety (**17**) was accompanied by a marked increase in enantioselectivity (68 : 32 e.r.), but curtailing rotational freedom of the group (**18**) or expanding the π-system (**19**) did not confer any further advantage (67 : 33 and 63 : 37 e.r., respectively). A switch to simple esters revealed that comparable enantioselectivity could be reached using the *i*Pr derivative (**20**; 67 : 33 e.r.), but further enlargement to the adamantyl ester (**21**) proved detrimental. When studying the influence of substituents with a second stereocenter, it was noted that incorporation of the D-menthol-derived (**22**) ester led to a boost in enantioselectivity (72 : 28 e.r.). In contrast, catalyst **23** containing the L-menthol motif gave marginally reduced selectivity (68 : 32 e.r.). To complete the catalyst editing study, amide-based catalysts were investigated (**24** and **25**), enabling enantioselectivities of up to 67 : 33 e.r. to be attained at ambient temperature. Notably, the L-proline-based catalyst (**26**) provided appreciable enantiocontrol (73 : 27) whereas the D-proline-based catalyst (**27**) proved less effective.

Having identified catalyst **26** as being a suitable candidate to facilitate the title transformation, the material was subjected to single crystal X-ray diffraction analysis.[18] The perspective shown in Fig. 1 allows the C_2-symmetry of the catalyst to be fully appreciated. In further optimizing the catalysis conditions, we were cognizant that the competing racemic pathway involving phenoxenium cation formation had to be suppressed.[14] Zhdankin and co-workers have elegantly demonstrated that the stability of I(III) species is greatly influenced by the *trans*-influence of the ligands.[19] Therefore, in an attempt to stabilize the iodonium-substrate complex, methanol was introduced into the reaction mixture to facilitate ligand exchange.[19] This led to an increase in enantioselectivity (entry 1, 80 : 20 e.r.), which is also in line with observations from Ishihara and co-workers,[20] but the yield was severely impacted due to methanol acting as

a competing nucleophile. Unsurprisingly, similar observations were made with ethanol (entry 2), whereas fluorinated alcohols proved detrimental to both the yield and enantioselectivity of the process (entry 3). Further evaluation of reaction media led us to explore ethers, which have been shown to improve the enantioselectivity of certain I(I)/I(III)-catalyzed fluorination processes.[16b,d] Gratifyingly, transitioning to Et₂O as the solvent (entry 4) resulted in an increased enantioselectivity of 80 : 20 e.r.: this could be further improved using MTBE (entry 5), leading to an enantiomeric ratio of 82 : 18. It is interesting to note that the beneficial effect of MTBE on the enantioselectivity was only observed for amide-based catalysts. In contrast, there was almost no change in enantioselectivity when using ester-based catalysts. Moreover, the introduction of ether solvents such as 1,4-dioxane (entry 6) had a negative impact on selectivity.

To further improve the enantioselectivity, the reaction mixture was cooled to 0 °C and stirred for 48 h (entry 7): this enhanced the enantioselectivity to 88 : 12 e.r. but had a severe impact on conversion. Increasing the amount of *m*CPBA to 4 eq. (entry 8) enhanced catalysis efficiency, and this could be further improved by modifying the ratio of solvent to amine : HF (0.35 mL MTBE, 0.65 mL amine : HF 1 : 4.0, entry 9). To further increase enantioselectivity, the reaction mixture was cooled to −5 °C (entry 10) which allowed the product to be obtained in 61% yield with an enantiomeric ratio of 87 : 13. Moreover, the dependence of enantioselectivity on the ratio of co-solvent to amine : HF could be further leveraged to reach 90 : 10 e.r. (entry 11). However, due to the reduction in yield observed at lower temperatures, the conditions listed in entry 10 were selected for the remainder of the study. Further cooling of the reaction to −10 °C (entry 12) led to incomplete conversion with only modest improvements in enantioselectivity.

Having identified optimized reaction conditions for the title process, a 2.0 mmol scale transformation was performed which enabled **9a** to be formed with the same yield (61%, 83 : 17 e.r.) which highlights the amenability of this transformation to scale-up (full details in the ESI†). To complement the bromo system **8a**, the corresponding halogen series was continued (Scheme 3): this was deemed prudent given the importance of chlorinated cyclohexadienes such as the pharmaceutical halometasone (see Scheme 1A). Exposing substrates **8b** and **8c** to the catalysis conditions delivered the expected products **9b** and **9c** with enantiomeric ratios of 87 : 13 and 85 : 15, respectively. The positive impact of the electron-withdrawing C2-substituent was fully leveraged by installing a triflate handle, thereby facilitating access **9d** with high levels of selectivity (92 : 8 e.r.). The importance of this substituent is evident from a direct comparison with the ONs derivative **9e** (85 : 15 e.r.). The acetate derivative behaved similarly (**9f**, 84 : 16 e.r.) as did the 2,4,5-trisubstituted phenols **8g** and **8h**, which furnished **9g** and **9h** with good levels of selectivity (85 : 15 e.r.) and in yields of up to 68%. Intriguingly, a switch to 2,3,4-trisubstitution patterns led to higher enantiomeric ratios as exemplified by cyclohexadienes **9i** and **9j** (up to 92 : 8 e.r. and up to 69%). Replacing the 4-methyl group with an ethyl group (**8a** and **8d** *versus* **8k** and **8l**) had no significant impact on enantioselectivity, furnishing product **9l**
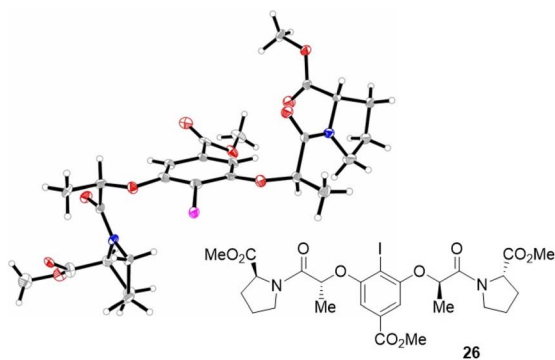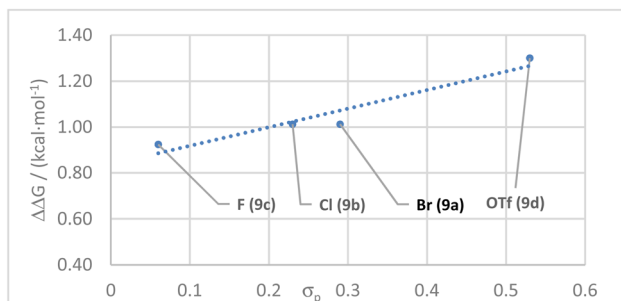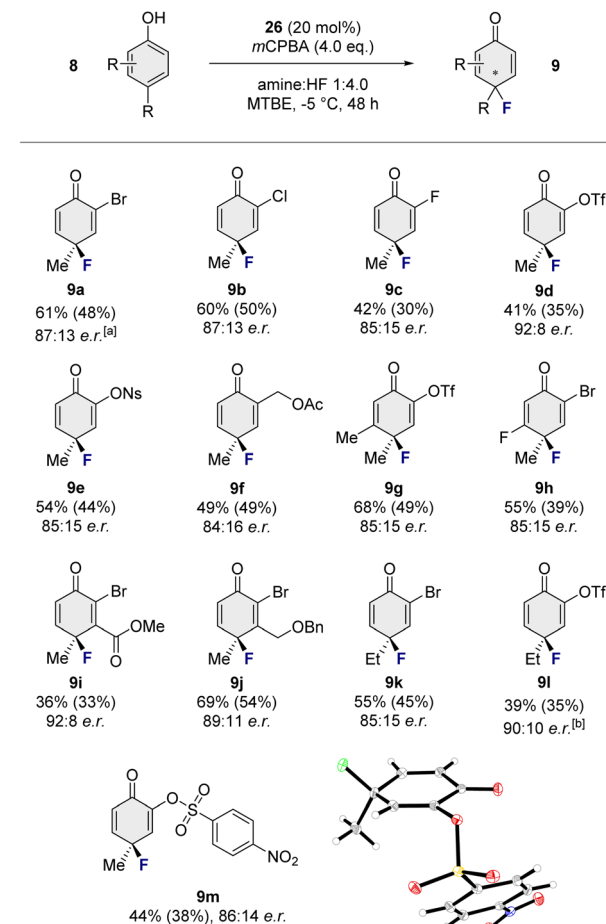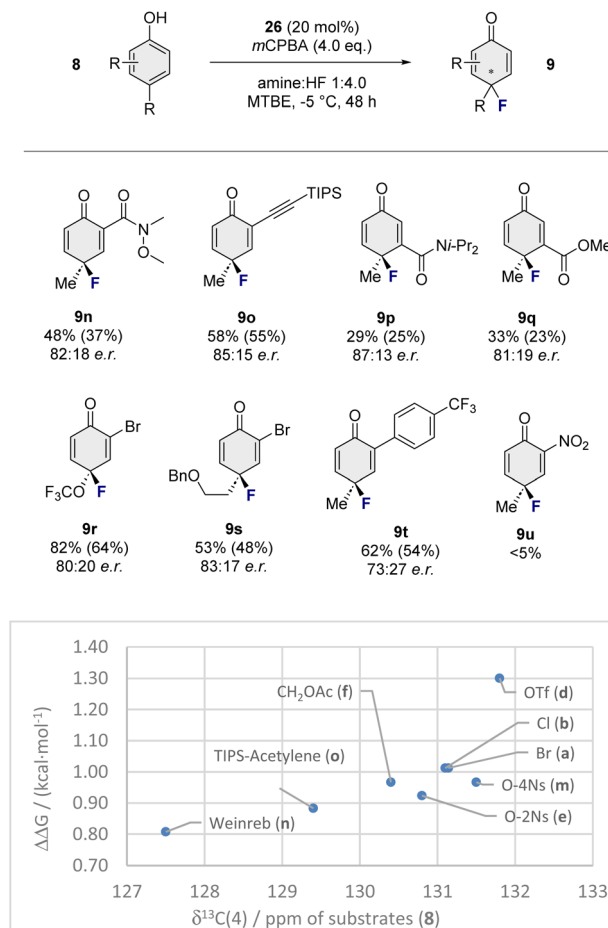

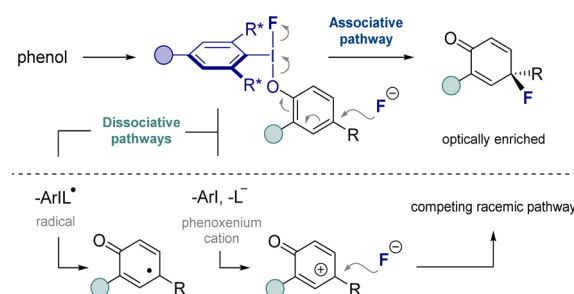Fig. 1 Crystal structure of catalyst **26**.[18]

Scheme 3 Exploring the scope of the asymmetric dearomatization of phenols. General conditions: phenol (0.2 mmol), **26** (20 mol%), amine : HF 1 : 4.0 (0.65 mL), MTBE (0.35 mL) and mCPBA (0.8 mmol), 48 h, −5 °C. Yield was determined by ^{19}F NMR using ethylfluoroacetate as the internal standard. Isolated yield given in parenthesis. Enantiomeric ratio (e.r.) was determined by chiral HPLC. Plot of substrate enantioselectivity *versus* σ_p. [a]Reaction at 2 mmol scale furnished **9a** in 61% yield (by ^{19}F NMR) and 83 : 17 e.r. [b]Reaction run for 72 h.

Scheme 4 Top: Exploring the functional group compatibility of the transformation. General conditions: phenol (0.2 mmol), **26** (20 mol%), amine : HF 1 : 4.0 (0.65 mL), MTBE (0.35 mL) and mCPBA (0.8 mmol), 48 h, −5 °C. Yield was determined by ^{19}F NMR using ethylfluoroacetate as the internal standard. Isolated yield given in parenthesis. Enantiomeric ratio (e.r.) was determined by chiral HPLC. Middle: A plot of $\Delta\Delta G$ (kcal mol^{-1}) of the reaction against the carbon shift of the substrate *para*-positions [δ^{13}C(4)]. Bottom: A postulated mechanistic scenario involving a competing dissociative pathway.

with good levels of selectivity (up to 90 : 10 e.r.). Gratifyingly, it was possible to obtain crystals of the sulfone derivative **9m**, allowing the absolute configuration of the product to be determined as (*S*) by means of X-ray diffraction.[21] It is interesting to note that the C–F bond length of 142 pm is comparable to that of other tertiary C–F bonds.[22] To investigate the possibility of phenoxenium cation involvement in a competing racemic side reaction, the Hammett parameters (σ_p) of selected *ortho*-
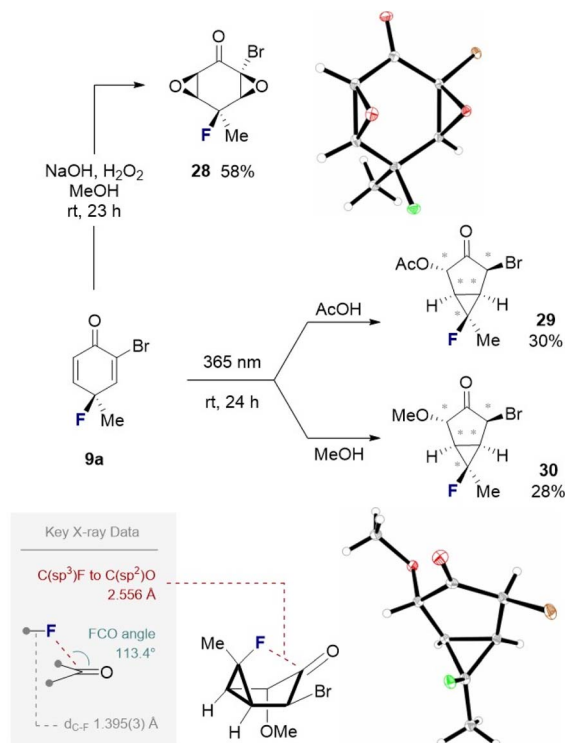
substituents from the 4-methyl-subsituted substrates was plotted against $\Delta\Delta G$.[23] This supports the experimental observations that more electron deficient substituents suppress phenoxenium ion formation and this manifests itself in higher levels of enantioselectivity.

Scheme 5 Top: Oxidation and photochemical rearrangement of **9a** to generate densely substituted ketones **28**, **29** and **30** with five contiguous stereocenters. Bottom: Observation of a C(sp^3)–F···C=O interaction (2.556 Å).

To further investigate the functional group tolerance of the reaction conditions, motifs such as Weinreb amides (**9n**) and TIPS protected acetylenes (**9o**) were incorporated, enabling the desired 1,4-cyclohexadienones to be generated with 82 : 18 e.r. and 85 : 15 e.r., respectively. Given that the asymmetric dearomatization of 3,4-disubstituted phenols is generally challenging,[12,24] it was gratifying to observe that products **9p** and **9q** could be obtained using this method. However, replacing the C4 (Me) substituent by OCF$_3$ (**9r**) or a pendant alkyl chain (**9s**) led to a reduction in enantioselectivity. This also holds for C2 aryl substituted systems as is evident from entry **9t**. Highly electron deficient substrates such as **8u** proved recalcitrant to oxidation. To place these experimental observations on a structural footing, the carbon shift of the substrate *para*-positions [δ^{13}C(4)] was plotted against the $\Delta\Delta G$ (kcal mol^{-1}); this was performed due to the lack of Hammett parameters for many of the substrate phenols. From this plot, a loose trend can be observed that links higher enantioselectivities with an increased shift of the carbon signal. These data, together with the plot of substrate enantioselectivity *versus* σ_p shown in Scheme 3, support the involvement of a dissociative (racemic) pathway competing with the enantioselective process.[14] This may explain why the inclusion of this challenging reaction in the ever-expanding I(I)/I(III) dearomatization inventory has not been achieved until now (Scheme 4, bottom), and stimulate further interest in this transformation.

To demonstrate the synthetic utility of the fluorinated cyclohexadienones generated in the study, compound **9a** was processed to a set of stereochemically rich products (Scheme 5).

Exposure to basic H$_2$O$_2$ proceeded in a highly stereoselective fashion with the methyl group ensuring facial selectivity to generate the di-epoxide **28** as the sole product of the reaction. The relative stereochemistry of the product was unambiguously established by X-ray analysis.[25] Inspired by the elegant work by Pirrung and Nunn on the photochemical rearrangements of quinone monoketals,[26] **9a** was irradiated at 365 nm for 24 h with the intention of inducing a di-π-methane rearrangement.[27] Under similar conditions using acetic acid or methanol as the solvent, the sole products of these reactions were the densely substituted cyclopentanones **29** and **30**, which were isolated as single diastereoisomers containing five contiguous stereogenic centers. The relative configuration of the product **30** was unequivocally established by single crystal diffraction.[28] It is interesting to note that the C(sp^3)–F of the cyclopropane occupies the concave face of the molecule and engages the carbonyl group in a manner that is highly reminiscent of n → π$_{C=O}$* interactions in 1,4-dicarbonyls.[29] The distance from the F atom to the C(sp^2) atom is 2.556 Å (and 2.956 Å to the center of the bond). This structural analysis contributes to the growing interest in understanding fluorine interactions with proximal carbonyl groups[30] and carbocations.[31]

Conclusion

Of the plenum of I(I)/I(III) catalysis-based dearomatization methods, the regio- and enantio-selective fluorination of phenols at C4 has proven to be a persistent challenge. Herein, we report a strategy that enables an array of diversely substituted substrates to be processed exclusively to the corresponding (C4) fluorinated cyclohexadienones (20 examples) with good levels of enantioselectivity (up to 92 : 08 e.r.). The structural trends observed in the course of this work are consistent with competitive (dissociate) pathways involving phenoxenium ions which compromise selectivity. Whilst this can be mitigated by carefully adjusting the reaction conditions, the prominence of this background reaction is likely the major contributory factor that has led to a lack of methods to enable the title transformation. The method complements the current state of the art in hydroxylation-enabled desymmetrization, thereby providing a platform to study the effects of OH to F bioisosterm. We envisage that this will be highly enabling given the venerable history of fluorinated cyclohexadienones in drug discovery, and the challenges associated with generating tertiary fluorides in a more general sense.[32] Finally, the synthetic utility of the products is demonstrated through a facile photochemical rearrangement to access fused cyclopentanones with five contiguous stereogenic centers. Structural analysis of this motif reveals an intriguing C(sp^3)–F···carbonyl interactions in which the distance of the F and C atoms is lower than the sum of the van der Waals radii.

Author contributions

TS and RG designed the project and TS, KS, DO, KM, LR and CGD conducted the experimental work. X-ray crystallographic

analyses were performed by CGD. TS, KS and RG wrote the manuscript.

Conflicts of interest

There are no conflicts to declare.

Acknowledgements

Notes and references

1 (a) S. P. Roche and J. A. Porco Jr, *Angew. Chem., Int. Ed.*, 2011, **50**, 4068; (b) C.-X. Zhuo, W. Zhang and S.-L. You, *Angew. Chem., Int. Ed.*, 2012, **51**, 12662; (c) C. Zheng and S.-L. You, *ACS Cent. Sci.*, 2021, **7**, 432; (d) W.-T. Wu, L. Zhang and S.-L. You, *Chem. Soc. Rev.*, 2016, **45**, 1570.

2 J. G. Allen and S. J. Danishefsky, *J. Am. Chem. Soc.*, 2001, **123**, 351.

3 J. H. Kim, D. H. Kim, S. H. Baek, H. J. Lee, M. R. Kim, H. J. Kwon and C.-H. Lee, *Biochem. Pharmacol.*, 2006, **71**, 1198.

4 (a) J. Cao, Q. Deng, L. Hu, X. Zhang and Y. Xiong, *Org. Biomol. Chem.*, 2022, **20**, 8104; (b) K. Kuramochi, K. Fukudome, I. Kuriyama, T. Takeuchi, Y. Sato, S. Kamisuki, K. Tsubaki, F. Sugawara, H. Yoshida and Y. Mizushina, *Bioorg. Med. Chem.*, 2009, **17**, 7227; (c) N. Maeda, Y. Kokai, S. Ohtani, H. Sahara, I. Kuriyama, S. Kamisuki, S. Takahashi, K. Sakaguchi, F. Sugawara, H. Yoshida, N. Sato and Y. Mizushina, *Biochem. Biophys. Res. Commun.*, 2007, **352**, 390.

5 Y. A. Jasem, T. Thiemann, L. Gano and M. C. Oliveira, *J. Fluorine Chem.*, 2016, **185**, 48.

6 World Health Organization, *World Health Organization model list of essential medicines: 22nd list (2021)*, World Health Organization, 2021, **https://iris.who.int/handle/10665/345533**, License: CC BY-NC-SA 3.0 IGO.

7 J. Fried, A. Borman, W. B. Kessler, P. Grabowich and E. F. Sabo, *J. Am. Chem. Soc.*, 1958, **80**, 2338.

8 (a) S. Meyer, J. Häfliger and R. Gilmour, *Chem. Sci.*, 2021, **12**, 10686; (b) P. Richardson, *Expert Opin. Drug Discovery*, 2021, **16**, 1261; (c) I. G. Molnár, C. Thiehoff, M. C. Holland and R. Gilmour, *ACS Catal.*, 2016, **6**, 7167; (d) E. P. Gillis, K. J. Eastman, M. D. Hill, D. J. Donnelly and N. A. Meanwell, *J. Med. Chem.*, 2015, **58**, 8315; (e) L. E. Zimmer, C. Sparr and R. Gilmour, *Angew. Chem., Int. Ed.*, 2011, **50**, 11860; (f) S. Purser, P. R. Moore, S. Swallow and V. Gouverneur, *Chem. Soc. Rev.*, 2008, **37**, 320; (g) D. O'Hagan, *Chem. Soc. Rev.*, 2008, **37**, 308; (h) K. Müller, C. Faeh and F. Diederich, *Science*, 2007, **317**, 1881.

9 (a) F. V. Singh, S. E. Shetgaonkar, M. Krishnan and T. Wirth, *Chem. Soc. Rev.*, 2022, **51**, 8102; (b) A. Parra, *Chem. Rev.*, 2019, **119**, 12033; (c) A. Yoshimura and V. V. Zhdankin, *Chem. Rev.*, 2016, **116**, 3328.

10 (a) O. Karam, J.-C. Jacquesy and M.-P. Jouannetaud, *Tetrahedron Lett.*, 1994, **35**, 2541; (b) O. Karam, A. Martin, M.-P. Jouannetaud and J.-C. Jacquesy, *Tetrahedron Lett.*, 1999, **40**, 4183; (c) O. Karam, A. Martin-Mingot, M.-P. Jouannetaud, J.-C. Jacquesy and A. Cousson, *Tetrahedron*, 2004, **60**, 6629.

11 (a) S. Stavber and M. Zupan, *Synlett*, 1996, 693; (b) S. Stavber, M. Jereb and M. Zupan, *Synlett*, 1999, 1375; (c) S. Stavber, M. Jereb and M. Zupan, *J. Phys. Org. Chem.*, 2002, **15**, 56; (d) I. Pravst, M. P. Iskra, M. Jereb, M. Zupan and S. Stavber, *Tetrahedron*, 2006, **62**, 4474.

12 T. Hashimoto, Y. Shimazaki, Y. Omatsu and K. Maruoka, *Angew. Chem., Int. Ed.*, 2018, **57**, 7200.

13 R. J. Phipps and F. D. Toste, *J. Am. Chem. Soc.*, 2013, **135**, 1268.

14 For selected examples, see: (a) A. Juneau, I. Lepage, S. G. Sabbah, A. H. Winter and M. Frenette, *J. Org. Chem.*, 2022, **87**, 14274; (b) K. Kraszewski, I. Tomczyk, A. Drabinska, K. Bienkowski, R. Solarska and M. Kalek, *Chem. – Eur. J.*, 2020, **26**, 11584; (c) T. Tang and A. M. Harned, *Org. Biomol. Chem.*, 2018, **16**, 8249; (d) T. Dohi, A. Maruyama, N. Takenaga, K. Senami, Y. Minamitsuji, H. Fujioka, S. B. Caemmerer and Y. Kita, *Angew. Chem., Int. Ed.*, 2008, **47**, 3787; (e) A. Pelter, A. Hussain, G. Smith and R. S. Ward, *Tetrahedron*, 1997, **53**, 3879.

15 For examples of C2-selective fluorinative dearomatization of phenols and related structures, see: (a) P. Wang, J. Wang, L. Wang, D. Li, K. Wang, Y. Liu, H. Zhu, X. Liu, D. Yang and R. Wang, *Adv. Synth. Catal.*, 2018, **360**, 401; (b) H. Egami, T. Rouno, T. Niwa, K. Masuda, K. Yamashita and Y. Hamashima, *Angew. Chem., Int. Ed.*, 2020, **59**, 14101; (c) M. Otsubo, K. Sakimoto, H. Egami and Y. Hamashima, *Tetrahedron*, 2021, **96**, 132355; (d) M. Thiele, T. Rose, M. Lõkov, S. Stadtfeld, S. Tshepelevitsh, E. Parman, K. Opara, C. Wölper, I. Leito, S. Grimme and J. Niemeyer, *Chem. – Eur. J.*, 2023, **29**, e202202953.

16 For selected examples, see: (a) Z.-X. Wang, K. Livingstone, C. Hümpel, C. G. Daniliuc and R. Gilmour, *Nat. Chem.*, 2023, **15**, 1515–1522; (b) J. Häfliger, L. Ruyet, N. Stübke, C. G. Daniliuc and R. Gilmour, *Nat. Commun.*, 2023, **14**, 3207; (c) Y.-J. Yu, J. Häfliger, Z.-X. Wang, C. G. Daniliuc and R. Gilmour, *Angew. Chem., Int. Ed.*, 2023, **62**, e202309789; (d) Y.-J. Yu, M. Schäfer, C. G. Daniliuc and R. Gilmour, *Angew. Chem., Int. Ed.*, 2023, **62**, e202214906; (e) J. Häfliger, O. O. Sokolova, M. Lenz, C. G. Daniliuc and R. Gilmour, *Angew. Chem., Int. Ed.*, 2022, **61**, e202205277; (f) M. Schäfer, T. Stünkel, C. G. Daniliuc and R. Gilmour, *Angew. Chem., Int. Ed.*, 2022, **61**, e202205508; (g) S. Meyer, J. Häfliger, M. Schäfer, J. J. Molloy, C. G. Daniliuc and R. Gilmour, *Angew. Chem., Int. Ed.*, 2021, **60**, 6430; (h) F. Scheidt, M. Schäfer, J. C. Sarie, C. G. Daniliuc, J. J. Molloy and R. Gilmour, *Angew. Chem., Int. Ed.*, 2018,

57, 16431; (*i*) I. G. Molnár and R. Gilmour, *J. Am. Chem. Soc.*, 2016, **138**, 5004.

17 J. C. Sarie, C. Thiehoff, R. J. Mudd, C. G. Daniliuc, G. Kehr and R. Gilmour, *J. Org. Chem.*, 2017, **82**, 11792.

18 X-ray data for **26** CCDC 2288991.†

19 (*a*) V. V. Zhdankin, R. M. Arbit, B. J. Lynch, P. Kiprof and V. G. Young, *J. Org. Chem.*, 1998, **63**, 6590; (*b*) V. V. Zhdankin, R. M. Arbit, M. McSherry, B. Mismash and V. G. Young, *J. Am. Chem. Soc.*, 1997, **119**, 7408; (*c*) M. Ochiai, T. Sueda, K. Miyamoto, P. Kiprof and V. V. Zhdankin, *Angew. Chem., Int. Ed.*, 2006, **45**, 8203.

20 M. Uyanik, T. Yasui and K. Ishihara, *Angew. Chem., Int. Ed.*, 2013, **52**, 9215.

21 X-ray data for **9m** CCDC 2288990.†

22 F. H. Allen, O. Kennard, D. G. Watson, L. Brammer, A. G. Orpen and R. Taylor, *J. Chem. Soc.*, 1987, S1–S19.

23 C. Hansch, A. Leo and R. W. Taft, *Chem. Rev.*, 1991, **91**, 165.

24 K. Muñiz and L. Fra, *Synthesis*, 2017, **49**, 2901.

25 X-ray data for **28** CCDC 2288992.†

26 M. C. Pirrung and D. S. Nunn, *Tetrahedron*, 1996, **52**, 5707.

27 (*a*) H. E. Zimmerman and D. Armesto, *Chem. Rev.*, 1996, **96**, 3065; (*b*) H. E. Zimmerman and J. M. Cassel, *J. Org. Chem.*, 1989, **54**, 3800; (*c*) S. S. Hixson, P. S. Mariano and H. E. Zimmerman, *Chem. Rev.*, 1973, **73**, 531.

28 X-ray data for **30** CCDC 2288993.†

29 (*a*) K. Livingstone, K. Siebold, S. Meyer, V. Martín-Heras, C. G. Daniliuc and R. Gilmour, *ACS Catal.*, 2022, **12**, 14507; (*b*) T. Neveselý, J. J. Molloy, C. McLaughlin, L. Brüss, C. G. Daniliuc and R. Gilmour, *Angew. Chem., Int. Ed.*, 2022, **61**, e202113600.

30 S. A. Harry, M. Kazim, P. M. Nguyen, A. Zhu, M. R. Xiang, J. Catazaro, M. Siegler and T. Lectka, *Angew. Chem., Int. Ed.*, 2022, **61**, e202207966.

31 (*a*) K. F. Hoffmann, A. Wiesner, C. Müller, S. Steinhauer, H. Beckers, M. Kazim, C. R. Pitts, T. Lectka and S. Riedel, *Nat. Commun.*, 2021, **12**, 5275; (*b*) M. D. Struble, M. G. Holl, M. T. Scerba, M. A. Siegler and T. Lectka, *J. Am. Chem. Soc.*, 2015, **137**, 11476; (*c*) M. D. Struble, M. T. Scerba, M. A. Siegler and T. Lectka, *Science*, 2013, **340**, 57.

32 (*a*) J.-A. Ma and D. Cahard, *Chem. Rev.*, 2004, **104**, 6119; (*b*) V. A. Brunet and D. O'Hagan, *Angew. Chem., Int. Ed.*, 2008, **47**, 1179; (*c*) Y. Zhu, J. Han, J. Wang, N. Shibata, M. Sodeoka, V. A. Soloshonok, J. A. S. Coelho and F. D. Toste, *Chem. Rev.*, 2018, **118**, 3887.